

# Rational Synthesis of Silver Vanadium Oxides/Polyaniline Triaxial Nanowires with Enhanced Electrochemical Property

Liqiang Mai,<sup>\*,†,‡</sup> Xu Xu,<sup>†</sup> Chunhua Han,<sup>†</sup> Yanzhu Luo,<sup>†</sup> Lin Xu,<sup>†</sup> Yimin A. Wu,<sup>§</sup> and Yunlong Zhao<sup>†</sup>

<sup>†</sup>State Key Laboratory of Advanced Technology for Materials Synthesis and Processing, WUT-Harvard Joint Nano Key Laboratory, Wuhan University of Technology, Wuhan 430070, China

<sup>‡</sup>Department of Chemistry and Chemical Biology, Harvard University, Cambridge, Massachusetts 02138, United States

<sup>§</sup>Department of Materials, University of Oxford, Parks Road, Oxford OX1 3PH, United Kingdom

**S** Supporting Information

**ABSTRACT:** We designed and successfully synthesized the silver vanadium oxides/polyaniline (SVO/PANI) triaxial nanowires by combining *in situ* chemical oxidative polymerization and interfacial redox reaction based on  $\beta$ -AgVO<sub>3</sub> nanowires. The  $\beta$ -AgVO<sub>3</sub> core and two distinct layers can be clearly observed in single triaxial nanowire. Fourier transformed infrared spectroscopic and energy dispersive X-ray spectroscopic investigations indicate that the outermost layer is PANI and the middle layer is Ag<sub>x</sub>VO<sub>(2.5+0.5x)</sub> ( $x < 1$ ), which may result from the redox reaction of Ag<sup>+</sup> and aniline monomers at the interface.

The presence of the Ag particle in a transmission electron microscopy image confirms the occurrence of the redox reaction. The triaxial nanowires exhibit enhanced electrochemical performance. This method is shown to be an effective and facile technique for improving the electrochemical performance and stability of nanowire electrodes for applications in Li ion batteries.

**KEYWORDS:**  $\beta$ -AgVO<sub>3</sub>, conducting polymer, triaxial nanowires, electrochemical property



Silver vanadium oxides (SVO) have drawn much attention since Ag<sub>2</sub>V<sub>4</sub>O<sub>11</sub> was used as the cathode active material in lithium primary batteries for implantable cardioverter defibrillators owing to its high energy density and long-term stability.<sup>1</sup>  $\beta$ -AgVO<sub>3</sub> has a higher Ag:V molar ratio, which is supposed to have better electrochemical performance.<sup>2</sup> However, few researchers have focused on its electrochemical performance and the modification methods in recent years.

Nanowires have attracted increasing interest because one-dimensional (1-D) nanomaterials can offer a range of unique advantages in electrochemical and energy related fields.<sup>3–5</sup> Complex nanostructures have been increasingly reported in recent years because they could offer better electrochemical performance than single-structured materials.<sup>6–10</sup> Among these complex structures, core/multishell nanowires have drawn much attention.<sup>11–14</sup> p-Si/i-Ge/SiO<sub>x</sub>/p-Ge core/multishell nanowires were prepared by Lieber's group for the field-effect transistor, whose high transconductance lead to improvements in transistor performance.<sup>13</sup> They also prepared core/multishell nanowires with an n-GaN core and In<sub>x</sub>Ga<sub>1-x</sub>N/GaN/p-AlGaN/p-GaN shells, which show the tunable emission from 365 to 600 nm and high quantum efficiencies.<sup>14</sup> To improve the electrochemical property, coaxial nanowires with conducting polymer shell have been widely studied.<sup>15–18</sup> Polyaniline (PANI) is one of the most used conducting polymers due to its high conductivity, chemical stability, facile process ability, ease of synthesis, and low cost. Recently, aniline was also used to synthesize PANI/silver nanocomposite

through a facile one-step redox reaction between Ag<sup>+</sup> and aniline monomers, which exhibits potential applications.<sup>19–22</sup>

In this work, combining the *in situ* chemical oxidative polymerization and the interfacial redox reaction between Ag<sup>+</sup> and aniline, we propose a rational route to synthesize SVO/PANI triaxial nanowires with enhanced electrochemical properties as cathode materials of a Li ion battery.

All chemicals were commercially available and used as received. A typical synthetic route is as follows:  $\beta$ -AgVO<sub>3</sub> nanowires were first synthesized by a simple hydrothermal reaction using AgNO<sub>3</sub> and NH<sub>4</sub>VO<sub>3</sub> at 180 °C for 24 h. The as-prepared  $\beta$ -AgVO<sub>3</sub> nanowires were dispersed in deionized water under stirring and ultrasonic vibration. Liquid aniline monomers with 50% weight percentage of  $\beta$ -AgVO<sub>3</sub> nanowires were slowly injected into the solution during vigorous magnetic stirring. After 12 h, ammonium persulfate with 1:1 mol ratio to monomer was then added to the solution. The mixture was allowed to react for another 12 h under constant stirring at room temperature. The resulting product was filtered and washed with deionized water and ethanol and then dried at 80 °C for 12 h to obtain SVO/PANI triaxial nanowires.

An X-ray diffraction (XRD) measurement was performed to investigate the crystallographic information using a D/MAX-III

**Received:** August 24, 2011

**Revised:** September 27, 2011

**Published:** October 11, 2011

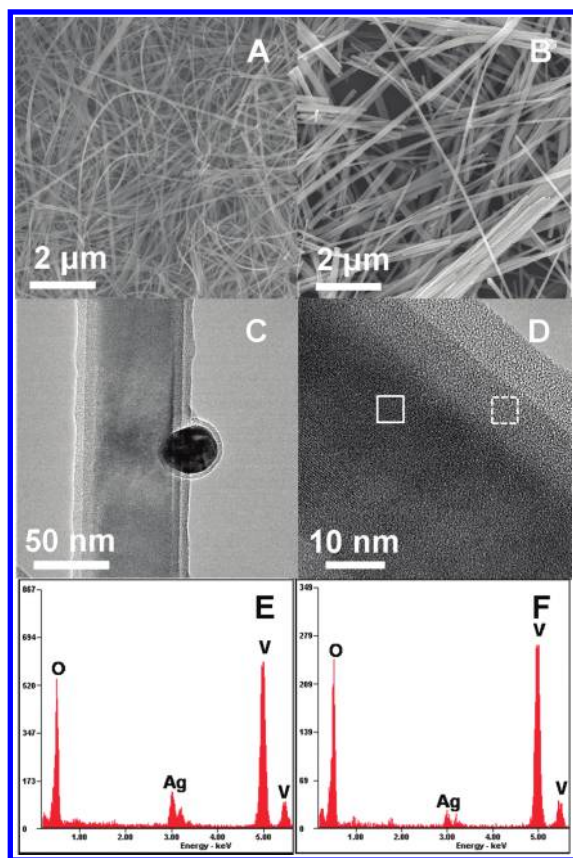


**Figure 1.** FESEM images of  $\beta$ -AgVO<sub>3</sub> nanowires (A) and SVO/PANI (B) triaxial nanowires. TEM and HRTEM images of SVO/PANI triaxial nanowires (C, D). EDS spectra of the selected areas in solid line (E) and dotted line (F) in panel D.

X-ray diffractometer with graphite-monochromatized Cu  $K\alpha$  radiation. Fourier transformed infrared (FTIR) spectra were recorded using the 60-SXB IR spectrometer to characterize the bonding properties. Field emission scanning electron microscopy (FESEM) images were collected with a Hitachi S-4800 at an acceleration voltage of 20 kV. Transmission electron microscopy (TEM), high-resolution transmission electron microscopy (HRTEM) images, and energy dispersive X-ray spectra (EDS) were recorded by using a JEM-2100F STEM/EDS microscope.

The electrochemical properties were carried out by assembly of coin cells with lithium pellet as the anode, 1 M solution of LiPF<sub>6</sub> in ethylene carbon (EC)/dimethyl carbonate (DMC) as electrolyte, and a pellet made of the active material, acetylene black, and poly(tetrafluoroethylene) (PTFE) in a 70:25:5 weight ratio as the cathode. Galvanostatic charge/discharge cycling was studied with a multichannel battery testing system (Neware). Cyclic voltammetry (CV) and electrochemical impedance spectrometry (EIS) were tested with an electrochemical workstation (Autolab Potentiostat 30).

Figure 1 shows the SEM and TEM images of  $\beta$ -AgVO<sub>3</sub> nanowires and SVO/PANI triaxial nanowires. Figure 1A shows the large quantities of bending  $\beta$ -AgVO<sub>3</sub> nanowires with the lengths of several tens of micrometers. Compared with  $\beta$ -AgVO<sub>3</sub> nanowires, the obtained SVO/PANI nanowires are shorter and thicker because of the stirring during the reaction and the PANI layer polymerized on the surface of nanowires (Figure 1B). Just as what we designed, typical triaxial nanowires with  $\beta$ -AgVO<sub>3</sub>

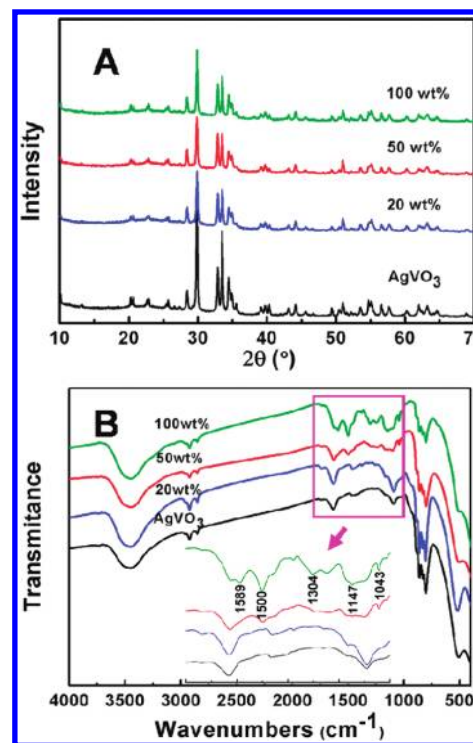


**Figure 2.** XRD (A) and FTIR (B) patterns of  $\beta$ -AgVO<sub>3</sub> nanowires and SVO/PANI nanowires with different adding weight of aniline.

core and two distinct layers can be obviously observed in TEM and HRTEM images (Figure 1C,D). The diameter of the triaxial nanowire is about 80 nm with the thickness of outermost PANI layer and middle layer both about 8 nm. Clear lattice fringes along the longitudinal direction of the nanowire with an interval of approximately 0.44 nm are observed, which corresponds to the  $d$  spacing of (400) lattice planes (Figure S1, Supporting Information). EDS spectra of the selected areas in the core (Figure 1E) and middle layer (Figure 1F) both indicate the presence of Ag, V, and O elements, which confirm that the middle layer of the triaxial nanowire is one form of the silver vanadium oxides existing between the  $\beta$ -AgVO<sub>3</sub> core and the PANI layer.

From Figure 1C we can also see a particle with a PANI layer attaching on the triaxial nanowire. The diameter is about 30 nm, and it is confirmed to be metallic silver, which is the product of the interfacial reaction between Ag<sup>+</sup> and aniline monomers. The formation of a silver particle has also been reported when Ag<sup>+</sup> reacted with aniline monomers.<sup>21,22</sup> It has been reported that metallic silver nanoparticles could *in situ* form under bombardment of high-energy electrons during TEM observation of  $\beta$ -AgVO<sub>3</sub>.<sup>23</sup> However, except for the PANI coating silver particles formed before TEM observation, no extra silver particles can be observed under the electron beam irradiation, which indicates that the structure stability of  $\beta$ -AgVO<sub>3</sub> is improved by the PANI coating.

Control experiments with different aniline amounts have also been carried out. With other synthetic parameters unchanged, when the aniline weight percentage of  $\beta$ -AgVO<sub>3</sub> nanowires changed from 50% to 20%, an obvious PANI layer was not observed on nanowires surface. When the aniline weight percentage was up to 100%, the PANI layer was much thicker and relatively uneven. In order to investigate the relationship between the structure and property of SVO/PANI nanowires,

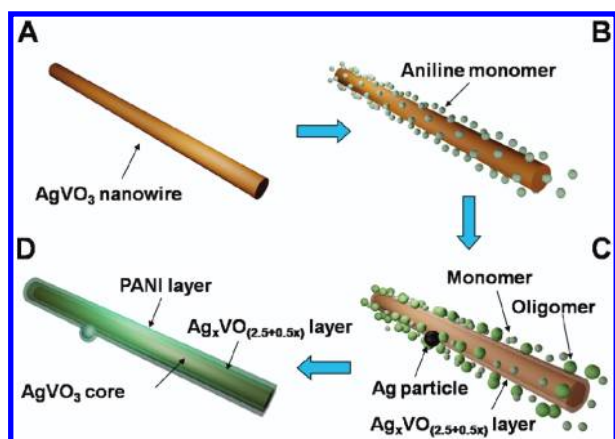


**Figure 3.** Schematic illustration of the formation of SVO/PANI triaxial nanowire.

XRD, FTIR, and battery performance of these two control samples were studied below for comparison.

XRD patterns of  $\beta$ - $\text{AgVO}_3$  nanowires and SVO/PANI nanowires with different aniline weights are shown in Figure 2A. All the diffraction peaks of as-prepared  $\beta$ - $\text{AgVO}_3$  nanowires can be readily indexed to pure phase of  $\beta$ - $\text{AgVO}_3$  with the monoclinic structure space group:  $I2/m$  (No. 12), JCPDS-ICDD Card No. 29-1154. No peaks from other phases have been detected, indicating that the products are of high purity. The characteristic peaks of SVO/PANI nanowires have a consistent position with pure  $\beta$ - $\text{AgVO}_3$ , whereas the peak density decreases with the increasing amount of aniline. The consistent peak position shows that the formation of PANI on nanowires surface does not dramatically destroy the structure of  $\beta$ - $\text{AgVO}_3$ , and the intensity decrease can be explained by the formation a PANI layer on the nanowire surface. The peaks of SVO/PANI nanowires have no shift, which indicates that the PANI did not intercalate into the interlayers of  $\beta$ - $\text{AgVO}_3$  but just forms on the surface of nanowires. The phase of metallic silver is not observed in XRD patterns of SVO/PANI nanowires, which may be because the amount of product silver is much less than the principal phase  $\beta$ - $\text{AgVO}_3$ .

Figure 2B displays FTIR spectra of  $\beta$ - $\text{AgVO}_3$  nanowires and SVO/PANI nanowires with different adding weight of aniline. For pure  $\beta$ - $\text{AgVO}_3$ , the characteristic absorption peaks are mainly in the range from 400 to 1000  $\text{cm}^{-1}$ , including the symmetric and asymmetric stretching vibration peaks of the V–O band and the stretching vibration mode of the V=O band. The peaks at 3448 and 1630  $\text{cm}^{-1}$  are the stretching and flexural vibrations of the O–H in free water, respectively.<sup>24</sup> All these peaks can also be observed in SVO/PANI nanowires, yet with weaker density. The characteristic peaks of PANI appear in SVO/PANI nanowires. The number and the density of the peaks increase with the amount of adding aniline. Taking 100 wt % SVO/PANI nanowires (aniline weight percentage of  $\beta$ - $\text{AgVO}_3$  is 100%) for instance, four characteristic peaks at 1147, 1304, 1500, and 1589  $\text{cm}^{-1}$  can be assigned as C–H plane-bending vibration, C–N stretching vibration, benzenoid ring stretching mode, and quinoid ring stretching mode, respectively. The characteristic peaks strongly show the successful polymerization of PANI on a nanowire surface. The band at 1043  $\text{cm}^{-1}$  can be designated as the split peak of C–H plane-bending vibration, indicating the strong interaction between the organic shell and inorganic core.<sup>25</sup>

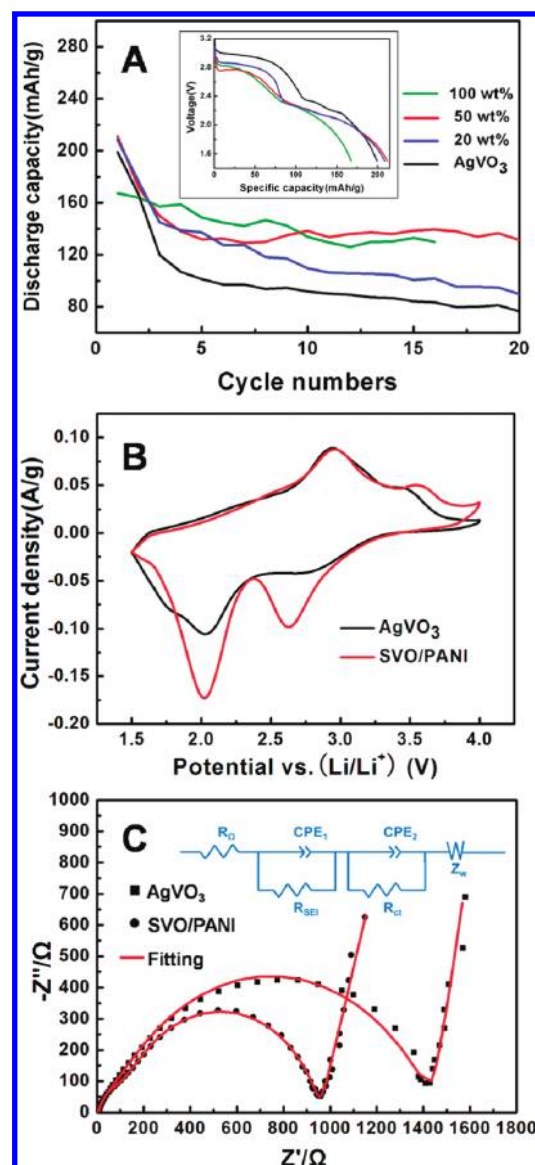


**Figure 4.** Capacity vs cycle number curves (A) and first discharge curves (inset of A) of  $\beta$ - $\text{AgVO}_3$  and SVO/PANI nanowires. CV curves (B) and ac-impedance spectra (C) of  $\beta$ - $\text{AgVO}_3$  nanowires and SVO/PANI triaxial nanowires.

Figure 3 is the schematic illustration of the formation of a triaxial nanowire. From the above results, it is understandable that the core of the triaxial nanowire is  $\beta$ - $\text{AgVO}_3$  and the outermost layer is PANI. When the liquid aniline monomers were added in the solvent, some of them first adsorbed on the surface of solid  $\beta$ - $\text{AgVO}_3$  nanowires and dispersed uniformly (Figure 3B). At the solid–liquid interface, a small amount of  $\text{Ag}^+$  dissolved from the  $\beta$ - $\text{AgVO}_3$  nanowire and took part in the oxidation reaction with aniline monomers, which lead to the formation of a middle  $\text{Ag}_x\text{VO}_{(2.5+0.5x)}$  ( $x < 1$ ) layer (Figure 3C). As a result, some of the aniline monomers transformed to liquid oligomers and small amounts of metallic silver particles formed. After the addition of ammonium persulfate, the polymerization was further carried out completely to form the PANI layer and the triaxial nanowire was finally obtained (Figure 3D). The formation of  $\text{Ag}_x\text{VO}_{(2.5+0.5x)}$  ( $x < 1$ ) is indicated by EDS spectra. Ag, V, and O elements are observed in both the core and the middle layer, while

the relative intensity of Ag peak in the middle layer is weaker than that in the core (Figure 1E,F), indicating the loss of Ag on a  $\beta$ -AgVO<sub>3</sub> nanowire surface. An Ag particle is also observed in the TEM image (Figure 1D), which confirms the occurrence of the redox reaction.

The higher capacity and better cycling stability of SVO/PANI nanowires were demonstrated as cathode materials of a rechargeable Li ion battery (Figure 4A). The batteries were cycled between 1.5 and 4 V at a charge/discharge current density of 30 mA/g. A 50 wt % SVO/PANI triaxial nanowire cathode possesses the highest initial and 20th discharge capacities, which are 211 and 131 mAh/g (with 20th cycle capacity retention of 62%), both higher than those of  $\beta$ -AgVO<sub>3</sub> nanowires, which are 199 and 76 mAh/g (with 20th cycle capacity retention of 41.7%). The rechargeable battery performance improvement can be attributed to SVO/PANI triaxial nanowires with uniform PANI shell offering better conductivity, less structure degradation, and less unwanted reactions during cycling, such as dissolution of transition metal in electrolyte.<sup>28–29</sup> Although 20 and 100 wt % SVO/PANI nanowires also have better battery performance than pristine  $\beta$ -AgVO<sub>3</sub> nanowires, the improvement is not as good as that with triaxial nanowires and the battery with 100 wt % SVO/PANI nanowire cathode has even been damaged after 16 cycles, indicating that the enhanced battery performance highly depends on the triaxial nanostructure. Our preliminary results also show that the battery performance of SVO/PANI triaxial nanowires may be improved by optimizing the synthetic parameters to adjust the thickness of the layers, the redox state of PANI, etc.

To further investigate the enhanced electrochemical performance of triaxial nanowires, CV and EIS tests of  $\beta$ -AgVO<sub>3</sub> nanowires and 50 wt % SVO/PANI triaxial nanowires were carried out. Figure 4B shows the CV curves of both samples for the first cycle at a scan rate of 0.2 mV/s. For both active materials, two pairs of cathodic/anodic peaks can be observed, corresponding to the lithium insertion/extraction reactions. For  $\beta$ -AgVO<sub>3</sub> nanowires, the oxidation/reduction peaks appear at 2.94/2.03 V and 3.45/2.66 V. The oxidation/reduction peaks of SVO/PANI nanowires are located at 2.96/2.02 V and 3.54/2.63 V, which are quite similar to  $\beta$ -AgVO<sub>3</sub> nanowires. However, it can be observed that the redox currents of SVO/PANI nanowires are much higher than those of  $\beta$ -AgVO<sub>3</sub> nanowires, which demonstrates faster kinetics and higher capacity of SVO/PANI triaxial nanowires. PANI can not only provide more pathways for charge transfer but also relieve the volume change during cycling, thus resulting in better electrochemical performance.<sup>30,31</sup>

The Nyquist plots of  $\beta$ -AgVO<sub>3</sub> nanowire and SVO/PANI triaxial nanowire electrodes are shown in Figure 4C, which both show two separated arcs in the high-frequency range and a sloped line in the low-frequency region. It is generally accepted that the two arcs are mainly caused by the formation of a solid electrolyte interface (SEI) film and the charge transfer reaction at the electrode/electrolyte interface, respectively. The straight line is associated with lithium ion diffusion in the electrode.<sup>32–34</sup> A simple equivalent circuit model (inset of Figure 4C) is built to analyze the impedance spectra of the two materials. In this circuit,  $R_{\Omega}$  presents the Ohmic resistance of the electrode system, which is due to the electrolyte and the cell components.  $R_{SEI}$  stands for the SEI resistance while  $R_{ct}$  represents the charge transfer resistance.  $CPE_1$ ,  $CPE_2$ , and  $Z_w$  are the SEI capacitance, double layer capacitance, and the Warburg impedance, respectively. The primary simulation parameters are listed in Table 1. It can be concluded from the Table 1 that  $R_{ct}$  of SVO/PANI decreased a lot compared with the pristine material, indicating much higher

**Table 1. The EIS Simulation Parameters of  $\beta$ -AgVO<sub>3</sub> Nanowires and SVO/PANI Triaxial Nanowires**

samples	$R_{\Omega}$ ( $\Omega$ )	$R_{SEI}$ ( $\Omega$ )	$R_{ct}$ ( $\Omega$ )
$\beta$ -AgVO <sub>3</sub>	4.653	49.4	1388
SVO/PANI	3.358	112.5	839.7

electronic conductivity with the PANI layer, which could result in a faster charge transfer reaction.  $R_{SEI}$  of SVO/PANI triaxial nanowires is higher than that of  $\beta$ -AgVO<sub>3</sub> nanowires, indicating the polymer coating can facilitate the formation of a SEI layer and prevent charge transfer through the layer. However, as the stable SEI layer would not shrink during the cathode lithiation/delithiation, it can act as a shelter for cathode material and improve the structure stability, which is good for the long-term stability of the electrode material.<sup>35–37</sup> Totally, the SVO/PANI triaxial nanowires possess lower resistance and faster kinetics than  $\beta$ -AgVO<sub>3</sub>, which agrees with the CV result.  $I$ - $V$  tests of  $\beta$ -AgVO<sub>3</sub> and SVO/PANI were performed via assembly of a thin-film device, and the result also indicates the conductivity increase of SVO/PANI triaxial nanowires (Figure S2, Supporting Information).

In summary, we successfully synthesized SVO/PANI triaxial nanowires with enhanced electrochemical performance by a one-step method based on  $\beta$ -AgVO<sub>3</sub> nanowires. The formation mechanism of the triaxial nanowires was proposed. CV investigation shows that the triaxial nanowires exhibit much higher current density than that of  $\beta$ -AgVO<sub>3</sub> nanowires, which indicates faster kinetics and higher capacity. The enhanced electrochemical performance of the triaxial nanowires may result from the decrease of the charge transfer resistance from 1388 to 839.7  $\Omega$ . This work demonstrates that our method is an effective and facile technique for synthesizing complex nanostructure and improving the electrochemical performance of nanowire electrodes for applications in Li ion batteries.

## ■ ASSOCIATED CONTENT

**S Supporting Information.** TEM image of a SVO/PANI triaxial nanowire, HRTEM images and FFT patterns of core and outer shell layer, and  $I$ - $V$  curves of  $\beta$ -AgVO<sub>3</sub> and SVO/PANI nanowires. This material is available free of charge via the Internet at <http://pubs.acs.org>.

## ■ AUTHOR INFORMATION

### Corresponding Author

\*E-mail: [mlq@cmliris.harvard.edu](mailto:mlq@cmliris.harvard.edu).

## ■ ACKNOWLEDGMENT

This work was partially supported by National Basic Research Program of China (973-program) (2012CB933000) and the National Nature Science Foundation of China (51072153), Program for New Century Excellent Talents in University (NCET-10-0661). Thanks to Professor C.M. Lieber of Harvard University, Professor Q.J. Zhang of Wuhan University of Technology, Professor Z.L. Wang of Georgia Institute of Technology and Professor J. Liu of Pacific Northwest National Laboratory for strong support and stimulating discussion. The authors want to thank Q. Gao and B. Hu of Wuhan University of Technology for their great contribution.

## REFERENCES

- (1) Takeuchi, K. J.; Marschilok, A. C.; Davis, S. M.; Leising, R. A.; Takeuchi, E. S. Silver Vanadium Oxides and Related Battery Applications. *Coord. Chem. Rev.* **2001**, *283*, 219–221.
- (2) Takeuchi, E. S.; Piliero, P. Lithium/Silver Vanadium Oxide Batteries with Various Silver to Vanadium Ratios. *J. Power Sources* **1987**, *21*, 133–141.
- (3) Tian, B.; Xie, P.; Kempa, T. J.; Bell, D. C.; Lieber, C. M. Single-Crystalline Kinked Semiconductor Nanowire Superstructures. *Nat. Nanotechnol.* **2009**, *4*, 824–829.
- (4) Dong, Y. J.; Tian, B. Z.; Kempa, T. J.; Lieber, C. M. Coaxial Group III-Nitride Nanowire Photovoltaics. *Nano Lett.* **2009**, *9*, 2183–2187.
- (5) Xu, S.; Qin, Y.; Xu, C.; Wei, Y.; Yang, R.; Wang, Z. L. Self-Powered Nanowire Devices. *Nat. Nanotechnol.* **2010**, *5*, 366–373.
- (6) Tian, B. Z.; Zheng, X.; Kempa, T. J.; Fang, Y.; Yu, N.; Yu, G.; Huang, J.; Lieber, C. M. Coaxial Silicon Nanowires as Solar Cells and Nanoelectronic Power Sources. *Nature* **2007**, *449*, 885–890.
- (7) Dong, Y. J.; Yu, G. H.; McAlpine, M. C.; Lu, W.; Lieber, C. M. Si/a-Si Core/Shell Nanowires as Nonvolatile Crossbar Switches. *Nano Lett.* **2008**, *8*, 386–391.
- (8) Mai, L. Q.; Yang, F.; Zhao, Y. L.; Xu, X.; Xu, L.; Luo, Y. Z. Hierarchical MnMoO<sub>4</sub>/CoMoO<sub>4</sub> Heterostructured Nanowires with Enhanced Supercapacitor Performance. *Nat. Commun.* **2011**, *2*, 381.
- (9) Mai, L. Q.; Xu, L.; Han, C. H.; Xu, X.; Luo, Y. Z.; Zhao, S. Y.; Zhao, Y. L. Electrospun Ultralong Hierarchical Vanadium Oxide Nanowires with High Performance for Lithium Ion Batteries. *Nano Lett.* **2010**, *10*, 4750–4755.
- (10) Jiang, X. C.; Tian, B. Z.; Xiang, J.; Qian, F.; Zheng, G. F.; Wang, H. T.; Mai, L. Q.; Lieber, C. M. Rational Growth of Branched Nanowire Heterostructures with Synthetically Encoded Properties and Function. *Proc. Natl. Acad. Sci. USA* **2011**, *108*, 12212–12216.
- (11) Hu, J. Q.; Bando, Y.; Liu, Y. W.; Sekiguchi, T.; Golberg, D.; Zhan, J. H. Epitaxial Heterostructures: Side-to-Side Si-ZnS, Si-ZnSe Biaxial Nanowires, and Sandwichlike ZnS-Si-ZnS Triaxial Nanowires. *J. Am. Chem. Soc.* **2003**, *125*, 11306–11313.
- (12) Hosono, E.; Wang, Y. G.; Kida, N.; Enomoto, M.; Kojima, N.; Okubo, M.; Matsuda, H.; Saito, Y.; Kudo, T.; Honma, I.; Zhou, H. S. Synthesis of Triaxial LiFePO<sub>4</sub> Nanowire with a VGCF Core Column and a Carbon Shell through the Electrospinning Method. *ACS Appl. Mater. Interfaces* **2010**, *2*, 212–218.
- (13) Lauthon, L. J.; Gudiksen, M. S.; Wang, D. L.; Lieber, C. M. Epitaxial Core–Shell and Core–Multishell Nanowire Heterostructures. *Nature* **2002**, *420*, 57–61.
- (14) Qian, F.; Gradecak, S.; Li, Y.; Wen, C. Y.; Lieber, C. M. Core/Multishell Nanowire Heterostructures as Multicolor, High-Efficiency Light-Emitting Diodes. *Nano Lett.* **2005**, *5*, 2287–2291.
- (15) Huang, X. H.; Tu, J. P.; Xia, X. H.; Wang, X. L.; Xiang, J. Y. Nickel Foam-Supported Porous NiO/Polyaniline Film as Anode for Lithium Ion Batteries. *Electrochem. Commun.* **2008**, *10*, 1288–1290.
- (16) Gowda, S. R.; Reddy, A. L. M.; Shaijumon, M. M.; Zhan, X. B.; Ci, L. J.; Ajayan, P. M. Conformal Coating of Thin Polymer Electrolyte Layer on Nanostructured Electrode Materials for Three-Dimensional Battery Applications. *Nano Lett.* **2011**, *11*, 101–106.
- (17) Li, G. C.; Zhang, C. Q.; Peng, H. R.; Chen, K. Z. One-Dimensional V<sub>2</sub>O<sub>5</sub>@Polyaniline Core-Shell Nanobelts Synthesized by An *In Situ* Polymerization Method. *Macromol. Rapid Commun.* **2009**, *30*, 1841–1845.
- (18) Li, L.; Qin, Z. Y.; Liang, X.; Fan, Q. Q.; Lu, Y. Q.; Wu, W. H.; Zhu, M. F. Facile Fabrication of Uniform Core-Shell Structured Carbon Nanotube-Polyaniline Nanocomposites. *J. Phys. Chem. C* **2009**, *113*, 5502–5507.
- (19) Bober, P.; Trchová, M.; Prokes, J.; Varga, M.; Stejskal, J. Polyaniline–Silver Composites Prepared by The Oxidation of Aniline with Silver Nitrate in Solutions of Sulfonic Acids. *Electrochim. Acta* **2011**, *56*, 3580–3585.
- (20) Gao, Y.; Shan, D. C.; Cao, F.; Gong, J.; Li, X.; Ma, H. Y.; Su, Z. M.; Qu, L. Y. Silver/Polyaniline Composite Nanotubes: One-Step Synthesis and Electrocatalytic Activity for Neurotransmitter Dopamine. *J. Phys. Chem. C* **2009**, *113*, 15175–15181.
- (21) Bober, P.; Stejskal, J.; Trchová, M.; Hromádková, J.; Prokes, J. Polyaniline-Coated Silver Nanowires. *React. Funct. Polym.* **2010**, *70*, 656–662.
- (22) Blinova, N. V.; Stejskal, J.; Trchová, M.; Sapurina, I.; Ciric-Marjanovic, G. The Oxidation of Aniline with Silver Nitrate to Polyaniline-Silver Composites. *Polymer* **2009**, *50*, 50–56.
- (23) Mai, L. Q.; Xu, L.; Gao, Q.; Han, C. H.; Hu, B.; Pi, Y. Q. Single-AgVO<sub>3</sub> Nanowire H<sub>2</sub>S Sensor. *Nano Lett.* **2010**, *10*, 2604–2608.
- (24) Song, J. M.; Lin, Y. Z.; Yao, H. B.; Fan, F. J.; Li, X. G.; Yu, S. H. Superlong β-AgVO<sub>3</sub> Nanoribbons: High-Yield Synthesis by A Pyridine-Assisted Solution Approach, Their Stability, Electrical and Electrochemical Properties. *ACS Nano* **2009**, *3*, 653–660.
- (25) Lai, C.; Li, G. R.; Dou, Y. Y.; Gao, X. P. Mesoporous Polyaniline or Polypyrrole/Anatase TiO<sub>2</sub> Nanocomposite as Anode Materials for Lithium-Ion Batteries. *Electrochim. Acta* **2010**, *55*, 4567–4572.
- (26) Mai, L. Q.; Dong, Y. J.; Xu, L.; Han, C. H. Single Nanowire Electrochemical Devices. *Nano Lett.* **2010**, *10*, 4273–4278.
- (27) Tarascon, J. M.; Armand, M. Issues and Challenges Facing Rechargeable Lithium Batteries. *Nature* **2001**, *414*, 359–367.
- (28) Wang, Y. G.; Wu, W.; Cheng, L.; He, P.; Wang, C. X.; Xia, Y. Y. A Polyaniline-Intercalated Layered Manganese Oxide Nanocomposite Prepared by an Inorganic/Organic Interface Reaction and Its High Electrochemical Performance for Li Storage. *Adv. Mater.* **2008**, *20*, 2166–2170.
- (29) Ahn, D.; Koo, Y. M.; Kim, M. G.; Shin, N.; Park, J.; Eom, J.; Cho, J.; Shin, T. J. Polyaniline Nanocoating on the Surface of Layered LiLi<sub>0.2</sub>Co<sub>0.1</sub>Mn<sub>0.7</sub>O<sub>2</sub> Nanodisks and Enhanced Cyclability as A Cathode Electrode for Rechargeable Lithium-Ion Battery. *J. Phys. Chem. C* **2010**, *114*, 3675–3680.
- (30) Ruffo, R.; Wessells, C.; Huggins, R. A.; Cui, Y. Electrochemical Behavior of LiCoO<sub>2</sub> as Aqueous Lithium-Ion Battery Electrodes. *Electrochem. Commun.* **2009**, *11*, 247–249.
- (31) Cui, C. J.; Wu, G. M.; Yang, H. Y.; She, S. F.; Shen, J.; Zhou, B.; Zhang, Z. H. A New High-Performance Cathode Material for Rechargeable Lithium-Ion Batteries Polypyrrole/Vanadium Oxide Nanotubes. *Electrochim. Acta* **2010**, *55*, 8870–8875.
- (32) Lee, J. W.; Popov, B. N. Electrochemical Intercalation of Lithium into Polypyrrole/Silver Vanadium Oxide Composite Used for Lithium Primary Batteries. *J. Power Sources* **2006**, *161*, 565–572.
- (33) Ramasamy, R. P.; Feger, C.; Strange, T.; Popov, B. N. Discharge Characteristics of Silver Vanadium Oxide Cathodes. *J. Appl. Electrochem.* **2006**, *36*, 487–497.
- (34) Aurbach, D.; Gamolsky, K.; Markovsky, B.; Salitra, G.; Gofer, Y.; Heider, U.; Oesten, R.; Schmidt, M. The Study of Surface Phenomena Related to Electrochemical Lithium Intercalation into Li<sub>x</sub>MO<sub>y</sub> Host Materials (M = Ni, Mn). *J. Electrochem. Soc.* **2000**, *147*, 1322–1331.
- (35) Hu, L. B.; Wu, H.; Gao, Y. F.; Cao, A. Y.; Li, H. B.; McDough, J.; Xie, X.; Zhou, M.; Cui, Y. Silicon–Carbon Nanotube Coaxial Sponge as Li-Ion Anodes with High Areal Capacity. *Adv. Energy Mater.* **2011**, *1*, 523–527.
- (36) Gnanaraj, J. S.; Thompson, R. W.; DiCarlo, J. F.; Abraham, K. M. The Role of Carbonate Solvents on Lithium Intercalation into Graphite. *J. Electrochem. Soc.* **2007**, *154*, 185–191.
- (37) Choi, N. S.; Yao, Y.; Cui, Y.; Cho, J. One Dimensional Si/Sn -Based Nanowires and Nanotubes for Lithium-Ion Energy Storage Materials. *J. Mater. Chem.* **2011**, *21*, 9825–9840.